Site-selective laser spectroscopy of $CaF_2:Pr^{3+}$ and $CaF_2:Pr^{3+},R^{3+}$ ($R^{3+}=Y^{3+}$, Gd^{3+}, Nd^{3+})

Brian M. Tissue and John C. Wright
Department of Chemistry, University of Wisconsin–Madison, Madison, Wisconsin 53706
(Received 4 June 1987)

Site-selective laser spectroscopy has been used to investigate the defect structure of a 0.1 mol % $Pr^{3+}:CaF_2$ crystal. Twenty-three distinct sites have been identified from the fluorescence spectra. Only three of the sites were found to be single-ion sites while the rest were assigned to be clusters of two or more ions. The single-ion sites are a C_{4v} site, which dominates the spectrum at 0.1 mol %, a cubic site, and a site of low symmetry. Of the 20 cluster sites identified, two sites undergo intracluster energy transfer at a rate slow enough to be directly observed.

INTRODUCTION

When Pr^{3+} ions are doped into fluorite crystals they substitute at dipositive Ca lattice positions and therefore require charge compensation to maintain overall neutrality. The charge compensation is provided by a local interstitial fluoride ion $(Pr_{Ca}\cdot F_i)^x$ or by a distant fluoride interstitial (F_i'). The different possible positions of the interstitial F^- will result in dopant ions in different crystallographic sites. Any association of defects containing a single rare-earth ion will be referred to as single-ion sites regardless of the number of associated F^- interstitials. Theoretical results of Corish, Catlow, Jacobs, and Ong[1] show that rare-earth sites compensated by a F_i' in nearest-neighbor (NN) interstitial positions are favored by small lattice constants and sites compensated by a F_i' in the next-nearest-neighbor (NNN) positions are favored by larger lattice constants. Therefore C_{4v} sites are predicted to predominate in CaF_2, C_{3v} sites to predominate in BaF_2, and both types are predicted in SrF_2. The size of the dopant ion was also shown to affect the position of interstitials, with larger dopants being more stable in C_{4v} sites than smaller dopants in the same host.

The assignment of dielectric relaxation lines for the rare earths in CaF_2, SrF_2, and BaF_2 agrees with these theoretical predictions.[2,3] The $R_{\rm I}$ and $R_{\rm IV}$ dielectric relaxation peaks seen in $CaF_2:Pr^{3+}$ are assigned as a C_{4v} single-ion site and a dimer site which has gettered an additional fluorine interstitial, respectively. The C_{4v} site (R_I) has been labeled the A site and is the dominant site at 0.1 mol % Pr^{3+}.[4,5] Since concentration dependence or annealing studies were not performed in the present work, none of the sites could be correlated to the $R_{\rm IV}$ line.

At higher dopant concentrations, e.g., $>10^{-3}$ mol %, the dopant ions and their associated F^- interstitials will aggregate to form cluster sites containing two or more rare-earth ions. Corish *et al.*[1] have shown that dimers of dopant ions with two interstitials in NN positions (see Fig. 2, Ref. 1) are stable relative to two isolated C_{4v} single-ion sites. In a subsequent paper Bendall, Catlow, Corish, and Jacobs[6] performed calculations on defect clusters containing more than two dopant ions. They showed that trimers, tetramers, and hexamers should also be stable when high enough concentrations are reached. In $CaF_2:R^{3+}$ the trimer was predicted to be more stable than the tetramer, and it was speculated that hexamers may form from the aggregation of two trimers.

It has generally been our observation in crystals with the fluorite structure that cluster sites will predominate when a dopant concentration of 0.05–1.0 mol % is reached, depending on the particular fluorite host and rare-earth ion.[7–15] The existence of higher-order clusters has been experimentally confirmed by three-body up conversion in Tb^{3+}, $Yb^{3+}:CaF_2$,[16] and $Pr^{3+}:CaF_2$.[5] It should be noted that the distribution of defect sites is also dependent on the thermal history of the crystal since the clusters can be dissociated at high temperatures and prevented from reforming by quenching rapidly.

The optical spectroscopic investigations of $CaF_2:Pr^{3+}$ reported in the literature[4,5,17–21] have been quite varied but have not yet produced a complete picture of the distribution of defect sites in this crystal. $CaF_2:Pr^{3+}$ has been studied by Duran and coworkers exciting the $^1D_2$ level and monitoring direct fluorescence.[4,17,18] They identified four sites which they assigned as follows: a, a single-ion site of C_{4v} symmetry; b' and b'', two ions in which they reported energy transfer between the ions; and c, a single-ion site of low symmetry. They also observed very fast fluorescence, which had a lifetime of ~ 1 μs, but they did not assign it as a site.[4]

Lezama *et al.*[5] have studied a 0.1 mol % $Pr^{3+}:CaF_2$ crystal exciting the $^1D_2$ level and monitoring up-converted $^3P_0\rightarrow{}^3H_4$ fluorescence. They were able to observe 10 sites which were each assigned as either a single ion or a cluster based on the temporal behavior of the up-converted fluorescence. Sites A, B, C, D, and E were assigned to be single-ion sites because the risetime and decay of the up-converted fluorescence was slow. The up conversion for these sites was proposed to occur via weak, long-range interactions between the sites. The remaining sites, F, G, H, I, and J; were assigned as clusters of two or more Pr^{3+} ions based on the very fast risetimes and fast decay of the up-converted fluorescence. The up conversion for these sites was proposed to occur

via a strong short-range interaction between ions in the same cluster site. Sites *F*, *H*, *I*, and *J* were found to contain more than two ions because they could up-convert light to the $^1S_0$ level when exciting $^1D_2$. Lezama *et al.*[5] reported their sites *A* and *G* were the same as sites *a* (C_{4v} single ion) and *b* (dimer), respectively, of Duran and co-workers.[4,17,18] We will show in this paper that site *G* is a different site from the *b* site of Duran. The *b* site actually corresponds to a site we have labeled *L*, which is spectrally very similar to site *G*.

Chrysochoos *et al.*[19] have studied the emission from $^3P_0$ in CaF_2:Pr^{3+} exciting at 476.505 nm with an argon-ion laser. They classified the lines in the emission spectra, based upon the concentration dependence of the relative intensities of the lines, into three groups: I, a single-ion site of C_{4v} symmetry; II, a dimer site; and III, a single-ion site of cubic symmetry. In comparing these fluorescence spectra to that of Duran, the only correlation is the group-II lines (dimer site) match site *a* of Duran (C_{4v} single-ion site).

CaF_2:Pr^{3+} has been extensively used by Macfarlane and coworkers[22–25] as a system for studying Pr^{3+}-F^- interactions and Pr^{3+} hyperfine interactions. They confirmed that the *A* site does have C_{4v} symmetry and that the ground state is a doublet with a $g_{\parallel}$ of 3.89.

The up-conversion experiments of Lezama *et al.*[5] clearly show that there are a large number of cluster sites which have their fluorescence quenched from the $^1D_2$ level. Because of their close proximity, the ions in a cluster are usually strongly coupled so that energy can be easily transferred from one ion in the cluster to another. The approximate energy levels of a single Pr^{3+} ion and a pair of Pr^{3+} ions are shown in Fig. 1. It is evident that when one ion in a cluster is excited to the $^1D_2$ level it can relax to the $^1G_4$ level by transferring some of its energy to another ion in the cluster. The ion receiving the energy is excited from the ground state to the $^3F_4$ level. This energy transfer process can be written as $(^1D_2,{}^3H_4)\rightarrow(^1G_4,{}^3F_4)$. It is this ion pair decay process that is responsible for the quenching of the $^1D_2$ fluorescence of the cluster sites. Up-converted fluorescence is observable from the clusters under intense excitation because a $(^1D_2,{}^1D_2)$ pair state cannot relax by the ion pair relaxation process described above.

Theoretical calculations predict there should be differences in the defect distribution in CaF_2 doped with the larger Pr^{3+} ion than with the smaller rare earths. Several questions still remain about this system, such as how many single ion sites are present, does a cubic site exist, and how important are the cluster sites? With the goal of obtaining a more complete understanding of the defect distribution and energy transfer in this system, we have studied a 0.1 mol% Pr^{3+}:CaF_2 crystal at 12 K. The $^3P_0$ and $^3P_1$ levels were chiefly studied because it is possible to observe direct fluorescence from all of the sites including the clusters. It can be seen in Fig. 1 that there is a gap between the $(^3P_0,{}^3H_4)$ pair state and the next lowest $(^1G_4,{}^1G_4)$ pair state so the rate of nonradiative decay in the clusters is not rapid enough to quench the $^3P_0$ fluorescence. Doubly-doped 0.01 mol% Pr^{3+},

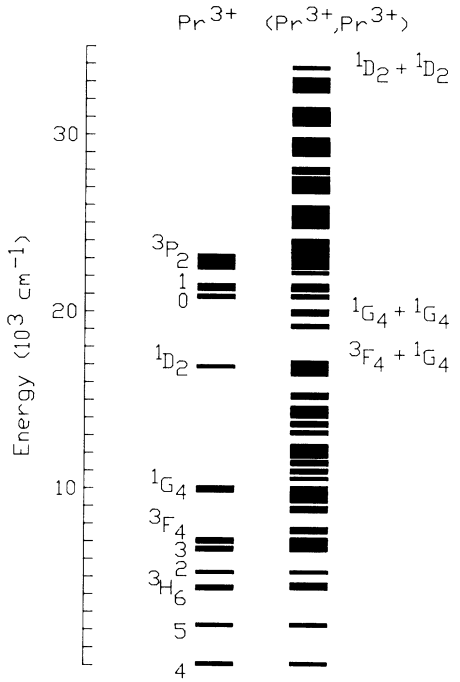

FIG. 1. Energy-level diagram for a single Pr^{3+} ion and the total possible energy states of both ions in a Pr^{3+} dimer in CaF_2. The energies for the $^3H_4$ thru $^1G_4$ levels were taken from Hargreaves (Ref. 21).

0.1%R^{3+}:CaF_2 precipitates ($R^{3+}=Y^{3+}$, Gd^{3+}, or Nd^{3+}) were also studied to try and confirm the assignment of the sites as either single ions or clusters. Codoping with Y^{3+} or Gd^{3+} should cause the lines of cluster sites to shift, since the Pr^{3+} in Y^{3+}-Pr^{3+} or Gd^{3+}-Pr^{3+} clusters will experience a slightly different crystalline field than in Pr^{3+}-Pr^{3+} clusters. Codoping with Nd^{3+} should completely quench Pr^{3+} fluorescence from cluster sites since Nd^{3+} will rapidly decay nonradiatively and fluoresce in the infrared. The spectra of single-ion sites should not be affected by any codopants.

EXPERIMENT

The 0.1 mol% Pr^{3+}:CaF_2 crystal was purchased from Optovac and used as received. The CaF_2:Pr^{3+},R^{3+} precipitates were prepared following the procedure developed by Gustafson and Wright.[26] Johnston[27] has shown that heating the precipitates in vacuum with PbF_2 oxygen getter produces a site distribution similar to that of the crystal. The precipitate was formed by slowly adding 20 mL of 0.3*M* NH_4F to 20 mL of a stirred $Ca(NO_3)_2$, RCl_3 solution. The precipitate was collected by filtering on 0.2 μm pore size paper and was annealed at 550° for 1.5 h under vacuum in the presence of PbF_2. A spectroscopic examination showed this procedure resulted in very little or no oxygen compensation.

The crystal or precipitate sample was mounted on the cold finger of a closed-cycle He refrigerator, which was capable of maintaining a temperature of 12 K. A 9-in

electromagnet, capable of fields from 0 to 25 kG, was available for Zeeman studies. A nitrogen laser pumped tunable dye laser with a typical bandwidth of 0.7 cm^{-1} was used as the excitation source. The excitation spectra of all sites was obtained by monitoring fluorescence with a low resolution (7-nm bandpass) $\frac{1}{4}$-m Fastie-Ebert monochromator, and an EMI 9785B PMT. A high-resolution 1-m Czerny-Turner monochromator and dry-ice-cooled EMI 9658R PMT were used to obtain fluorescence spectra of individual sites that were selectively excited with the dye laser. Spectra were obtained with a current to voltage converter and/or amplifier, gated integrator, and strip chart recorder. Fluorescence transients were recorded with a LeCroy TR8818 100 MHz transient recorder interfaced to an IBM PC AT computer and LeCroy Catalyst signal-averaging software.

RESULTS AND DISCUSSION

The excitation spectra in the region of 428–508 nm, monitoring fluorescence from all sites, is shown in Fig. 2. No transitions were observed in the regions of 450–460 or 482–508 nm. The lines were assigned by tuning the laser to each line and scanning the $^3P_0 \rightarrow {}^3F_2$ fluorescence spectrum. Excitation lines with the identical fluorescence spectrum and lifetime were assigned to the same site. The lines labeled by primed letters in the excitation spectra are not different sites but indicate different temporal behavior from the unprimed letters. The *E*-*E'* and *S*-*S'* sites will be discussed more fully in a section on energy transfer. The fluorescence lifetimes for each site are listed in Table I.

The $^3P_0 \rightarrow {}^3F_2$ fluorescence spectra for each site are shown in Fig. 3. The $^3P_0 \rightarrow {}^3H_4$ fluorescence spectra are shown in Fig. 4 for those sites which could be excited in the 462–472-nm region or excited by up conversion via the $^1D_2$ level. The sites have been labeled following the notation begun by Lezama *et al.*[5] Lines in the fluorescence spectra from other sites, which appear because of accidental overlap in excitation, have been labeled explicitly in the spectra.

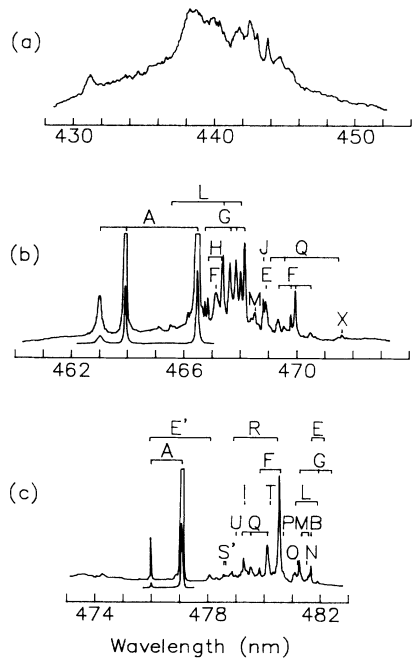

FIG. 2. Excitation spectra of the $^3H_4 \rightarrow {}^3P_{0,1,2}$ and $^1I_6$ region monitoring fluorescence from all sites with a gate width of 50 μs for the gated detection.

Three sites, *H*, *J*, and *X*, were not observed in the 475–483-nm excitation region but were observed in the 462–472-nm region. Sites *H* and *J* have $^3P_0 \rightarrow {}^3H_4$ fluorescence lines at 480.7 and 480.5 nm, respectively, but any *H* or *J* excitation lines in the 475–483-nm region are probably obscured by more intense lines from other sites. For site *X*, however, the $^3H_4 \rightarrow {}^3P_0$ excitation line which should appear at 477.6 nm was not observed. Two sites, *C* and *D*, were only observed when exciting by up conversion via the $^1D_2$ level. *C* and *D* are probably very minor sites which are obscured by stronger lines in the excitation spectra.

Previous work[22] has shown that site *A* has C_{4v} symmetry. Only one line should be observed in the region of the $^3H_4 \rightarrow {}^3P_0$ transition for a single ion, but site *A* clearly has two excitation lines at 476.0 and 477.1 nm. In order to determine the nature of these two lines their Zeeman splittings were measured. A magnetic field of 25 kG was applied parallel to a [111] axis so the Zeeman splittings of all the C_{4v} sites are equivalent. The resulting spectra are shown in Fig. 5. The $^3P_0 \rightarrow {}^3F_2$ fluorescence spectrum shows no splittings so the fluorescing level at 477.1 nm must not split. The splitting of 2.5 cm^{-1} in the lines at 476.0 and 477.1 nm must, therefore, be due to the ground-state splitting. This splitting agrees with that predicted from the value of $g_\parallel$ of the ground state measured by Macfarlane *et al.*[22] The lines at 463.0, 463.9, and 466.4 nm have widths of $\sim$4 cm^{-1} so a splitting of 2.5 cm^{-1} is not resolvable, although they are noticeably broadened. The 8-cm^{-1} splitting in the quartet at 476.0 and the 4-cm^{-1} splitting in the doublet at 466.4 nm are due to splittings in the excited-state levels. The 8-cm^{-1} splitting of the line at 476.0 nm could arise only if this line is a $^1I_6$ level. A splitting of 4.05 cm^{-1} is expected for the doubly degenerate $^3P_1$ line. The line at 466.4 nm is probably this line but it cannot be definitely assigned as $^3P_1$ since a $^1I_6$ line could also have a splitting this large. The unsplit lines at 463.0, 463.9, and 477.1 nm could be either $^3P_0$, $^3P_1$, or $^1I_6$ lines. We will continue to label the fluorescing level of each site as $^3P_0$ although this assignment is not definitive.

As can be seen in Table I site *X* has the longest lifetime of any site. The spectra of site *X* are also distinctly different, Fig. 6 shows the excitation spectrum and expanded $^3P_0 \rightarrow {}^3F_2$ and $^3P_0 \rightarrow {}^3H_4$ fluorescence spectra. The phonon sidebands at 657.0 and 495.5 nm in the $^3P_0 \rightarrow {}^3F_2$ and $^3P_0 \rightarrow {}^3H_4$ fluorescence spectra are the lines which Chrysochoos *et al.*[19] observed and assigned as site *I*. Phonon sidebands are present in the spectra of site *X* of comparable or greater intensity to the purely electronic transitions. No phonon sidebands of

TABLE I. Lifetimes and assignment of sites in 0.1 mol % Pr^{3+}:CaF_2.

Site	Lifetime (μs)	Number of $^3F_2$ Levels	Site assignment (minimum number of ions in cluster)	Evidence for assignment as a cluster
A	95.4± 4.9	2	C_{4v} single ion	d
B	42.5± 4.2	5	(cluster ?)[b]	e
C		5	(cluster ?)[b]	e
D		5	(cluster ?)[b]	e
E	42.8± 4.2[a]	4	cluster (2)	e,f
E'	23.5± 2.4	4		
F	17.6± 1.8	5	cluster (3)[c]	e,g
G	1.3± 0.4	5	cluster (2)	e,g
H	0.7± 0.3	5	cluster (3)[c]	e,g
I	1.1± 0.4	5	cluster (3)[c]	e,g
J	0.5± 0.2	6	cluster (3)[c]	e,g
L	48.8± 4.9	4	single ion	d
M	48.0± 4.8	5	(cluster ?)[b]	h
N	41.3± 4.1	9	cluster (2)	i
O	27.7± 2.7	8	cluster (2)	i
P	25.2± 2.5	7	cluster (2)	i
Q	21.7± 2.2	5	cluster (2)	g
R	4.5± 0.9	12	cluster (3)	g,i
S-S'	1.6± 0.5[a]	7	cluster (2)	f,g,i
T	1.2± 0.4	5	cluster (2)	g
U	0.6± 0.4	8	cluster (2)	g,i
X	647 ±32	2	O_h single ion	d

[a]Some fluorescence lines show a risetime.
[b]Assignment is not definitive.
[c]Based on the observation of three-body up conversion (Ref. 5).
[d]Not applicable.
[e]Efficient up conversion.
[f]Energy transfer observed between the ions in the cluster.
[g]Short $^3P_0$ lifetime.
[h]No fluorescence observed from $^1D_2$ as in the clusters.
[i]More than $2J+1$ levels in $^3F_2$.

significant intensity were observed for any of the other sites. The long lifetime and intense phonon structure has led us to assign site *X* as a single ion of cubic symmetry.

The symmetry of site *X* was confirmed by measuring the Zeeman splitting as a function of orientation in the magnetic field. A crystal was visually oriented from the (111) cleavage planes and was polished flat on a (110) face. Rotating around a [110] axis allowed all three major crystallographic axes, [100], [110], and [111], to be rotated parallel to the magnetic field. The field strength was 25 kG and the crystal was rotated in increments of 10°. Figure 7 shows the Zeeman pattern of the excitation line for the magnetic field parallel to each axis. The monochromator was set on the broad fluorescence phonon sideband at 495.5 nm so that no orientations would be selectively monitored. As can be seen in Fig. 7 there are no changes in the position or number of Zeeman lines for different orientations, as expected for a cubic site. The changes in relative ratios of the lines occur because of changes in the polarization selection rules since a magnetic field along [100], [110], and [111] axes lowers the symmetry of the ion from O_h to C_{4h}, C_{2h}, and C_{3i}, respectively. The cubic symmetry is responsible for the weak electronic transitions because the inversion symmetry forbids electric dipole transitions and only magnetic dipole transitions are allowed, which are inherently weaker. The polarization of the Zeeman lines is consistent with their assignment as magnetic dipole transitions.[28] The phonon sidebands are relatively intense compared to the electronic transitions because the phonon breaks the inversion symmetry and electric dipole transitions become allowed. The cubic site could not be observed exciting the $^1D_2$ level, probably because the transition is too strongly forbidden.

Most of the rest of this discussion will deal with assigning the rest of the sites as either single ions or clusters. A site can be identified as a cluster if it has more than the maximum number of $2J+1$ lines in any level. Because of the uncertainty of the assignment of levels in the excitation spectra, no conclusions can be unambiguously drawn from the number of lines in these spectra. However, the $^3F_2$ manifold appears to be isolated and it can be seen in the $^3P_0 \rightarrow {}^3F_2$ fluorescence spectra in Fig. 3 (and tabulated in Table I) that sites *J*, *N*, *O*, *P*, *R*, *S-S'*, and *U* have more than the maximum of five lines allowed for one ion. More than five lines are observed when the $^3P_0$ levels of the two (or more) ions in the cluster have similar energies so that both ions fluoresce.

Sites can also be identified as clusters if they show

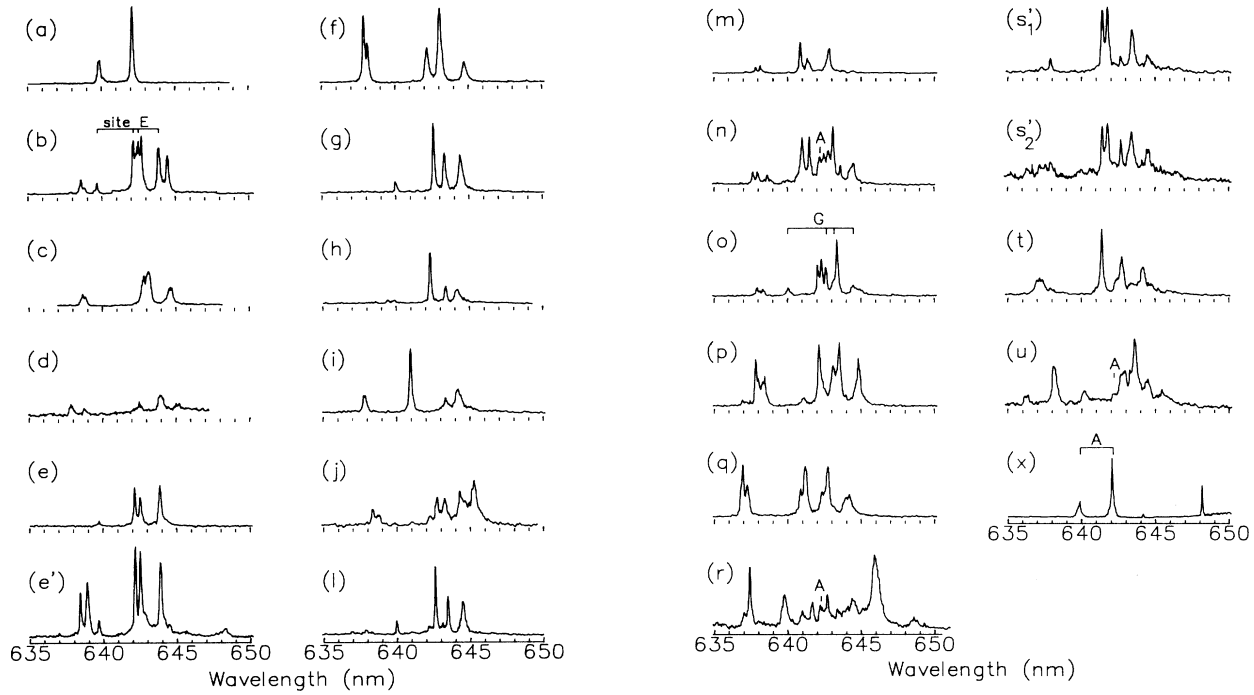

FIG. 3. $^3P_0 \rightarrow {}^3F_2$ fluorescence spectra of each individual site. The excitation wavelengths (in nm) to obtain these spectra were: (a) 476.0, (b) 481.7, (c) 594.0 ($^1D_2$), (d) 593.0 ($^1D_2$), (e) 481.7 (e') 478.1, (f) 480.6, (g) 481.3, (h) 466.8, (i) 479.3, (j) 468.8, (l) 481.1, (m) 481.4, (n) 481.6, (o) 481.2, (p) 480.7, (q) 480.2, (r) 478.9, (s_1') 478.56, (s_2') 478.62, (t) 480.3, (u) 479.0, (x) 471.6.

manifestations of strong interaction with a neighboring ion. Such manifestations include energy transfer, efficient up conversion, and fast nonradiative decay as evidenced by a short lifetime. Two sites, *E-E'* and *S-S'*, undergo energy transfer between the ions of the cluster at a rate slow enough to be observed. This is somewhat unusual for R^{3+} ions in fluorites, although energy transfer has been directly observed in the *K* site of $SrF_2:Er^{3+}$.[8,29]

When the excitation lines labeled *E* at 481.7 or 482.2 nm (the 482.2-nm line is a hot band) are excited, the $^3P_0 \rightarrow {}^3F_2$ fluorescence spectrum in Fig. 3(e) is observed.

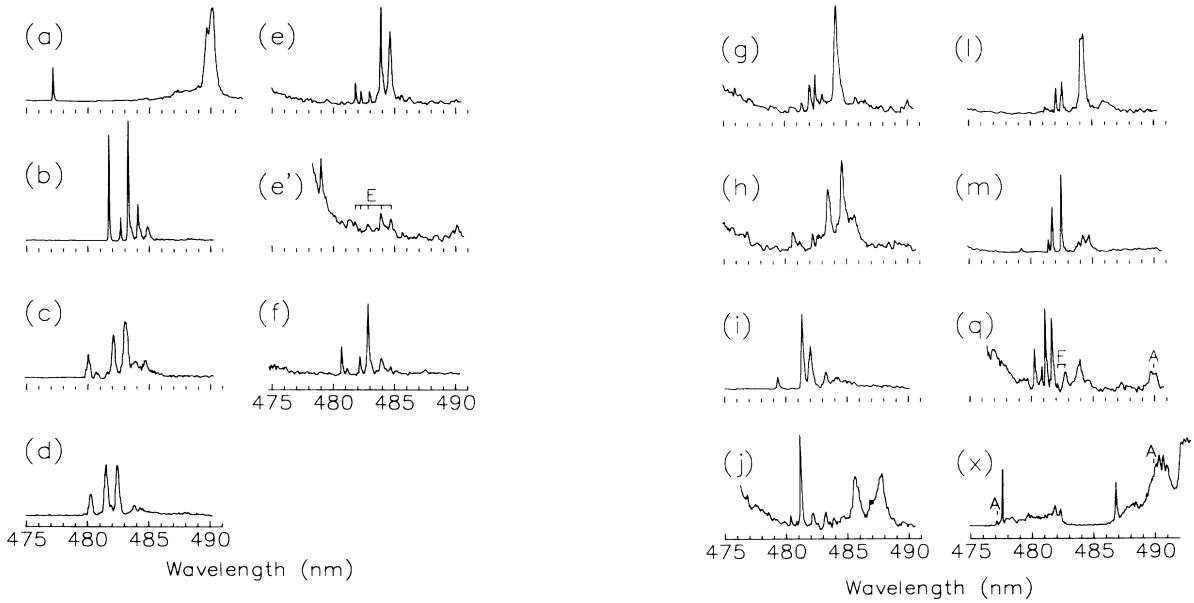

FIG. 4. $^3P_0 \rightarrow {}^3H_4$ fluorescence spectra of those sites which could be excited in the 462–472-nm region or excited by up conversion via $^1D_2$. The excitation wavelengths (in nm) used to obtain these spectra were: (a) 461.9, (b) 590.9, (c) 594.1, (d) 593.0, (e) 468.9, (e') 475.9, (f) 470.0, (g) 466.7, (h) 466.8, (i) 591.5, (j) 468.8, (l) 467.4, (m) 468.5, (q) 469.6, (x) 471.6.

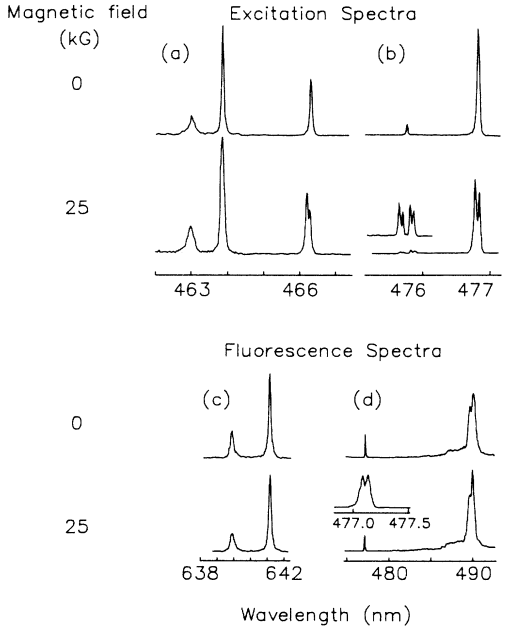

FIG. 5. Spectra of site A at 0 and 25 kG: (a) and (b) are excitation spectra monitoring fluorescence at 490.0 nm and (c) and (d) are fluorescence spectra exciting at 463.9 nm.

The fluorescence lines have the exponential decay shown in Fig. 8(a) with a lifetime of 42.8 μs. When the excitation lines labeled E' at 475.9 or 478.1 nm are excited, two sets of lines are observed in fluorescence, the E fluorescence lines and a new set E'. The E' fluorescence lines have the exponential decay shown in Fig. 8(b) with a lifetime of 23.5 μs while the E fluorescence lines show

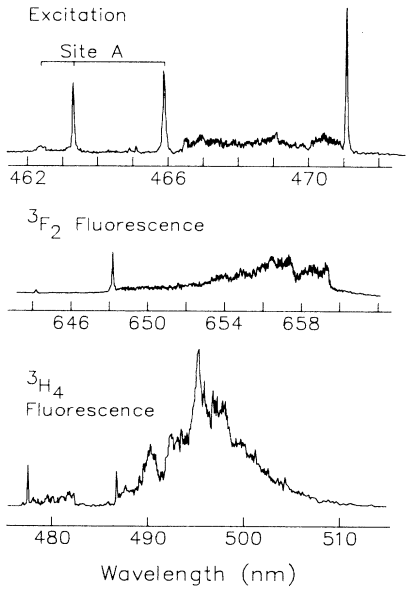

FIG. 6. Excitation and fluorescence spectra of site X. (a) Excitation spectrum monitoring fluorescence at 648.2 nm, (b) $^3P_0 \rightarrow {}^3F_2$, and (c) $^3P_0 \rightarrow {}^3H_4$ fluorescence spectra exciting at 471.6 nm.

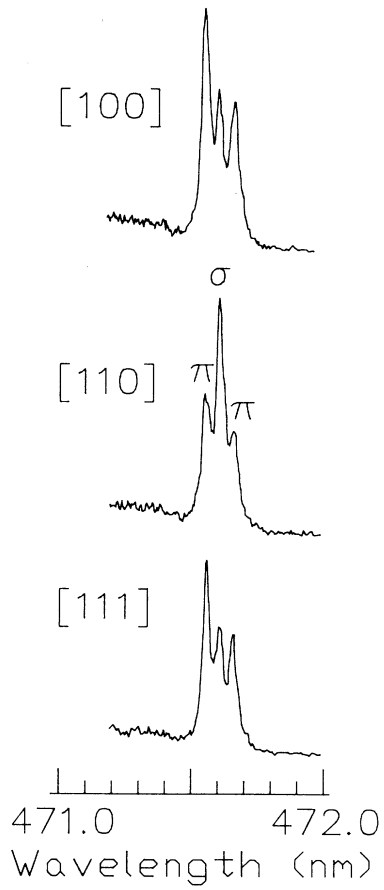

FIG. 7. The excitation spectrum of site X at 25 kG as a function of orientation in the magnetic field. Fluorescence was monitored at 495.5 nm.

a rise time and then decay as shown in Fig. 8(c).

These transients indicate that E and E' are ions in two distinct sites within a single cluster. When the higher energy E' ion is excited, fluorescence is observed from both E' and E because the energy transfer rate from E' to E is comparable to the radiative rate from E'.

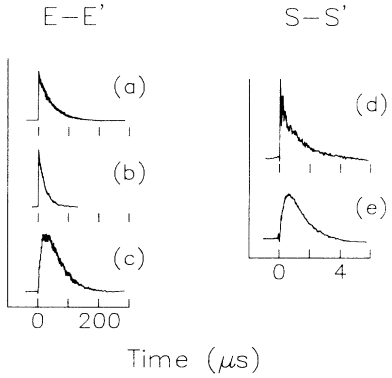

FIG. 8. The fluorescence transients of sites E-E' and S-S' as described in the text. The respective excitation and fluorescence wavelengths (in nm) for obtaining these transients are as follows: (a) 481.7 and 643.8, (b) 478.1 and 638.9, (c) 478.1 and 642.2, (d) 478.62 and 642.7, and (e) 478.62 and 641.4.

Fluorescence from the E ion therefore shows a risetime corresponding to the decay of the E' ion. The transient in Fig. 8(c) can be fit to a function of the form $(e^{-t/\tau_1}-e^{-t/\tau_2})$ with a τ_1 of 40 μs and a τ_2 of 20 μs. τ_1 and τ_2 correspond to the lifetimes of the E and E' ions, respectively, and are within experimental error of the lifetimes of E and E' measured directly.

Site S-S' shows slight changes in the relative ratios of some lines in the $^3P_0 \rightarrow {}^3F_2$ fluorescence spectrum, depending on which of the two excitation lines at 478.56 or 478.62 nm is excited, as seen for Fig. 3 [(s_1') and (s_2')]. When the $^3P_0 \rightarrow {}^3F_2$ fluorescence line at 642.7 nm is monitored, an exponential decay with a lifetime of 1.6 μs is observed as shown in Fig. 8(d). If the line at 641.4 nm is monitored, a transient with the functionality $(e^{-t/\tau_1}-e^{-t/\tau_2})$, where τ_1 is 1.5 μs and τ_2 is 0.4 μs, is observed as shown in Fig. 8(e). The same transients are observed for these fluorescence lines regardless of which excitation line is excited.

The risetime in the fluorescence transient when monitoring the 641.1-nm fluorescence line shows that the ion labeled S, responsible for this line is excited by energy transfer from another ion. The analysis of the transient in Fig. 8(e) indicates that the S ion should have an exponential decay of $\sim$0.4 μs. No fluorescence lines with a lifetime of 0.4 μs were observed and it is assumed that the S excitation line is obscured by more intense lines from other sites. An exponential decay with a lifetime of 1.6 μs is observed when the fluorescence line at 642.7 nm is monitored. This decay matches the τ_1 in the transient of the 641.1-nm fluorescence line so the ion(s), labeled S', responsible for the fluorescence lines at 642.7 nm is also the ion which is transferring energy to the S ion. There are two S' excitation lines at 478.56 and 478.62 nm. These two lines could arise from either two distinct ions or from two closely spaced levels of one ion. It is not possible to determine if the splitting of 0.06 nm seen in the excitation lines is also present in the $^3P_0 \rightarrow {}^3F_2$ fluorescence spectrum since the width of the fluorescence lines is $\sim$0.15 nm. The only evidence which distinguishes the two excitation lines is the change in the relative ratio of the 642.7-nm fluorescence line (ion S') to the other lines (ion S). Excitation of the line at 478.56 nm provides more efficient energy transfer than excitation at 478.62 nm as demonstrated by the ratio of the 641.4-nm line to the 642.7-nm line being greater. There is no reason that excitation of one or the other of two closely spaced levels of a single ion should cause differences in the fluorescence spectrum. Therefore the two lines have been assigned as arising from two distinct ions, labeled S_1' and S_2', with one of the ions undergoing slightly more efficient energy transfer to the S ion. The difference between the S_1' and S_2' ions is assumed to be too small to resolve in the $^3P_0 \rightarrow {}^3F_2$ fluorescence spectrum.

Lezama *et al.*[5] assigned sites F, H, I, and J to clusters containing more than two Pr^{3+} ions based on their fast up-conversion rate and their up conversion to the $^1S_0$ level. They assigned site G as a dimer because of its fast up-conversion rate to $^3P_0$ and negligible up-conversion rate to $^1S_0$. The short $^3P_0$ lifetimes of these sites, listed in Table I, are consistent with their assignment as clusters. Given the short lifetimes of sites Q and T, 21.7 and 1.2 μs, respectively, they also have been assigned as clusters. Lezama *et al.*[5] assigned sites A, B, C, D, and E to single-ion sites based on their lower rate of up conversion. While site A has been confirmed to be a C_{4v} single-ion site, site E (E-E') has been shown to be a cluster. It is difficult to assign sites B, C, and D as single ions or clusters. Figure 2 of this paper and the $^3H_4 \rightarrow {}^1D_2$ absorption spectrum of Lezama *et al.*[5] show that sites B, C, and D exist in the crystal in relatively low concentrations. One would expect the up conversion of single ion sites to scale approximately with the concentration of those sites since up conversion occurs by excitation of two nearby ions of the same site symmetry. Sites B, C, and D undergo comparable or more efficient up conversion than site A (site B has the strongest $^3H_4 \rightarrow {}^1D_2$ excitation line when monitoring up-converted fluorescence), even though they are present in much lower concentrations than site A. Given this inconsistency, sites B, C, and D may also be clusters. Minor cluster sites can appear anomalously intense in up conversion if they have small energy mismatches and/or strong coupling between the ions.

Lezama *et al.*[5] reported the G site was the same as the b site of Duran and coworkers,[4,17,18] but we find that site L is the same as Duran's b site. The $^1D_2 \rightarrow {}^3H_4$ fluorescence spectrum of Duran's b site and the $^3P_0 \rightarrow {}^3H_4$ fluorescence spectra of sites G and L are compared by matching the crystal-field levels of $^3H_4$ as shown in Fig. 9. It is evident that levels for Duran's b

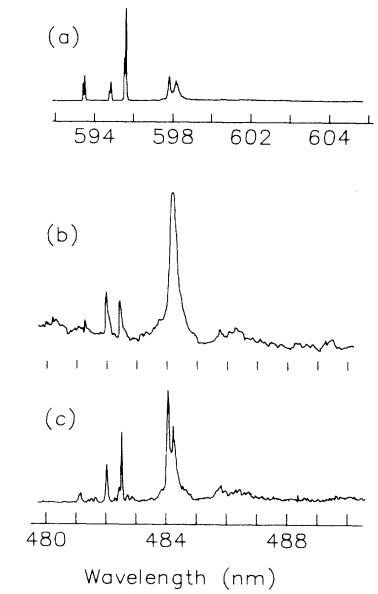

FIG. 9. Comparison of the $^1D_2 \rightarrow {}^3H_4$ fluorescence spectrum of the b site observed by Duran (Refs. 4, 17, and 18) to the $^3P_0 \rightarrow {}^3H_4$ fluorescence spectra of sites G and L. (a) $^1D_2 \rightarrow {}^3H_4$ fluorescence spectrum of the b site exciting at 593.5 nm, (b) and (c) $^3P_0 \rightarrow {}^4H_4$ fluorescence spectra of sites G and L exciting at 468.1 and 467.4 nm, respectively.

site correspond to those of site L. The confusion results because the fluorescence spectra of sites G and L are very similar. The $^3H_4 \rightarrow {}^3P_0$ excitation lines of sites G and L occur at 481.3 and 481.1 nm, respectively. The $^3H_4 \rightarrow {}^1D_2$ excitation spectrum of site G has two lines at 593.48 and 593.46 nm, which are not completely resolved, and a line at 590.8 nm; while site L has three lines at 593.47, 593.40, and 590.4 nm. Site L has a $^1D_2$ lifetime of 325 μs, comparable to site A's $^1D_2$ lifetime of 510 μs. We assign site L as a single-ion site on the basis of the fact that the $^1D_2$ fluorescence from site L is not quenched as it is for ions in clusters. The spectral similarities of sites G and L suggest that the ions in these sites experience the same crystal field. Since site G has been shown to be a dimer, it is reasonable to assign site G to consist of two equivalent ions which have the same

Duran and coworkers[4,17,18] assigned the b lines to correspond to two separate sites, b' and b''. In particular the $^1D_2 \rightarrow {}^3H_4$ fluorescence lines at 16719 and 16729 cm^{-1} were assigned to the b' and the b'' sites, respectively, on the basis of different fluorescence transients.[18] We did not observe any lines in the $^3P_0$ or $^3P_1$ levels that caused different relative intensities or transients for the lines of site L. It is possible that the effects Duran and coworkers attributed to energy transfer are the result of spectral overlap with short-lived fluorescence from the G site. Since the $^1D_2$ levels of sites G and L overlap, the $^1D_2 \rightarrow {}^3H_4$ fluorescence lines of site G would overlap with the site L fluorescence lines to the $^3H_4$ Stark levels of 0, 39, and 123 cm^{-1}.

In an effort to determine if any of the remaining sites may be single-ion sites, CaF_2 precipitates were prepared codoped with both Pr^{3+} and either Gd^{3+}, Y^{3+}, or Nd^{3+}. Figure 10 shows the excitation spectra, monitoring fluorescence from all sites, for the precipitate samples. Several differences are evident between the spectra of the 0.1 mol% Pr^{3+}:CaF_2 precipitate and the crystal. Only a few of the sites identified in the crystal were observed in the precipitate and a broad absorption band is seen around 479 nm. An oxygen compensated site appears in the precipitate and is observed as a shoulder on the short-wavelength side of the site-A line at 476 nm. Codoping with Gd^{3+} or Y^{3+} had very drastic effects on both the positions and relative intensities of lines in the spectra. Site A is the only site which is identifiable in all of the spectra. Codoping with Nd^{3+} produced a spectrum in which only site A appears.

The sites seen in the 0.1 mol% Pr^{3+}:CaF_2 precipitate are probably the most stable sites and it can be seen in Fig. 10(a) that site A dominates the spectrum. The short anneal time and relatively low temperature will hinder the formation of clusters since the rate of cation mobility will be slower. The most noticeable difference is that site F, which contains at least three ions and has a strong excitation line at 480.6 nm in the crystal, does not appear in the precipitate. The differences between the precipitate and the crystal are probably due to the differences in the annealing of the two samples. While the spectra confirm that site A is a single-ion site, no

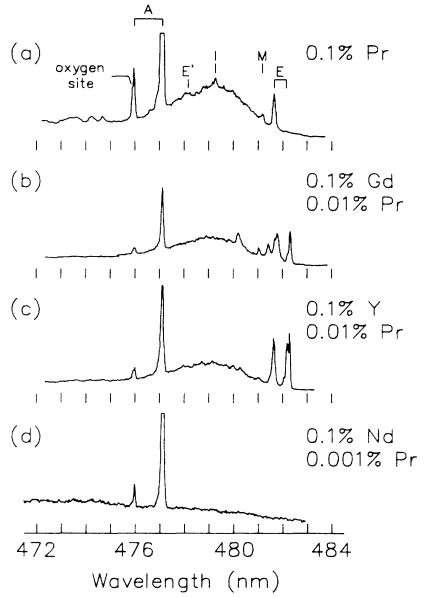

FIG. 10. Excitation spectra of the doped CaF_2 precipitates: (a) 0.1 mol% Pr^{3+}:CaF_2; (b) 0.01 mol% Pr^{3+}, 0.1 mol% Gd^{3+}:CaF_2; (c) 0.01 mol% Pr^{3+}, 0.1 mol% Y^{3+}:CaF_2; and (d) 0.001 mol% Pr^{3+}, 0.1 mol% Nd^{3+}:CaF_2. The $\frac{1}{4}$-m monochromator was used to collect fluorescence from all sites and the gated integrator was used with a gate of 50 μs at a delay of 30 μs after the laser fired.

conclusions can be drawn about the other sites since they did not all appear in the 0.1 mol% Pr^{3+}:CaF_2 precipitate. The spectra do show a trend in the importance of the cluster sites as the size of the dopant ion is changed. The site distribution in the doubly-doped samples will be controlled by the higher-concentration rare earth (Gd^{3+} or Y^{3+}). It can be seen in Figs. 10(a)–10(c) that the relative intensity of the cluster sites to site A is greatly increased in the precipitates codoped with the smaller ions Gd^{3+} and Y^{3+}.

The excitation spectra in Fig. 1 can be compared to the absorption spectra of 1.0 mol% Pr^{3+}:CaF_2 of Bhola[20] and Hargreaves.[21] While their lines could not be definitively correlated with sites, it is evident that site A is quite diminished compared to the other sites at 1 mol% Pr^{3+}. The concentration dependence of site A is shown in Fig. 5 (for the $^3P_0 \rightarrow {}^3H_5$ transition) of Chrysochoos *et al.*[19] The relative concentration of site A increases up to ~0.01 mol% and then drops off at higher concentrations. The assignments of sites by Chrysochoos *et al.*[19] were somewhat misinterpreted because of a limited concentration range and overlap of the sites in the regions of the spectra they had selected.

CONCLUSIONS

The assignment of each site as a cluster or single ion is summarized in Table I. Only three sites have been assigned as single ions: A (the C_{4v} site), L (a site of low

symmetry), and X (the cubic site). The number of lines in the $^3P_0 \rightarrow {}^3F_2$ fluorescence spectra of each site shows that there is no trigonal site in this system since a C_{3v} site would have three levels in the $^3F_2$ manifold.[30]

This work has shown that the defect distribution of $CaF_2:Pr^{3+}$ is more complex than previously thought, and is similar to other $CaF_2:R^{3+}$ systems. With the exception of the lack of a C_{3v} site it is especially similar to $CaF_2:Er^{3+}$, which contains cubic, C_{4v} and C_{3v} single-ion sites and 17 distinct cluster sites.[31] The absence of a C_{3v} site in $CaF_2:Pr^{3+}$ is consistent with the theoretical calculations of Corish *et al.*,[1] who predicted that the trigonal site should be unfavorable for larger lanthanide dopants.

Given the large number of sites found in the crystal it is difficult to explain the simplicity of the dielectric relaxation spectrum. The fluorescence spectra of the clusters show many similarities so it is possible that all of the cluster sites, which have a dipole moment, are very similar and together make up the R_{IV} relaxation.

Several very interesting sites were identified in this crystal which may be worthy of further study. Site G has been determined to be a cluster of equivalent ions which has very similar crystal-field splittings to the single-ion site L. Thus a determination of the symmetry of site L may also determine the microscopic structure of the cluster G. Two sites, E-E' and S-S', were found to be clusters in which energy transfer between the ions can be directly observed. Site E-E' may be a suitable cluster in which to study the mechanism of the nonresonant energy transfer. The energy transfer would be predicted to occur by a resonant two-phonon-assisted Orbach process since Stark levels exist in the $^3H_4$ manifold which provide real electronic levels for phonon scattering.[32]

ACKNOWLEDGMENTS

This work was supported by the National Science Foundation (Division of Materials Research) under Grant No. DMR-85-13705.

[1] J. Corish, C. R. A. Catlow, P. W. M. Jacobs, and S. H. Ong, Phys. Rev. B **25**, 6425 (1982).
[2] C. Andeen, D. L. Link, and J. Fontanella, Phys. Rev. B **16**, 3762 (1977).
[3] C. G. Andeen, J. J. Fontanella, M. C. Wintersgill, P. J. Welcher, R. J. Kimble, Jr., and G. E. Matthews, J. Phys. C **14**, 3557 (1981).
[4] J. Kliava, P. Evesque, and J. Duran, J. Phys. C **11**, 3357 (1978).
[5] A. Lezama, M. Oriá, and C. B. de Araujo, Phys. Rev. B **33**, 4493 (1986).
[6] P. J. Bendall, C. R. A. Catlow, J. Corish, and P. W. M. Jacobs, J. Solid State Chem. **51**, 159 (1984).
[7] D. R. Tallant, D. S. Moore, and J. C. Wright, J. Chem. Phys. **67**, 2897 (1977).
[8] M. D. Kurz and J. C. Wright, J. Lumin. **15**, 169 (1977).
[9] M. P. Miller and J. C. Wright, J. Chem. Phys. **68**, 1548 (1978).
[10] S. Mho and J. C. Wright, J. Chem. Phys. **79**, 3962 (1983).
[11] S. Mho and J. C. Wright, J. Chem. Phys. **81**, 1421 (1984).
[12] M. B. Seelbinder and J. C. Wright, Phys. Rev. B **20**, 4308 (1979).
[13] S. Mho and J. C. Wright, J. Chem. Phys. **77**, 1183 (1982).
[14] J. R. Wietfeldt and J. C. Wright, J. Chem. Phys. **83**, 4210 (1985).
[15] F. J. Weesner, J. C. Wright, and J. J. Fontanella, Phys. Rev. B **33**, 1372 (1986).
[16] M. B. Seelbinder and J. C. Wright, J. Chem. Phys. **75**, 5070 (1981).
[17] P. Evesque, J. Kliava, and J. Duran, J. Lumin. **18/19**, 646 (1979).
[18] R. H. Petit, P. Evesque, and J. Duran, J. Phys. C **14**, 5081 (1981).
[19] J. Chrysochoos, P. W. M. Jacobs, M. J. Stillman, and A. V. Chadwick, J. Lumin. **28**, 177 (1983).
[20] V. P. Bhola, Phys. Status Solidi B **68**, 667 (1975).
[21] W. A. Hargreaves, Phys. Rev. B **6**, 3417 (1972).
[22] R. M. Macfarlane, D. P. Burum, and R. M. Shelby, Phys. Rev. B **29**, 2390 (1984).
[23] D. P. Burum, R. M. Shelby, and R. M. Macfarlane, Phys. Rev. B **25**, 3009 (1982).
[24] R. M. Macfarlane, D. P. Burum, and R. M. Shelby, Phys. Rev. Lett. **49**, 636 (1982).
[25] R. M. Macfarlane, D. P. Burum, and R. M. Shelby, Opt. Lett. **6**, 593 (1981).
[26] F. J. Gustafson and J. C. Wright, Anal. Chem. **49**, 1680 (1977).
[27] M. V. Johnston, Ph.D thesis, University of Wisconsin, 1980 (unpublished).
[28] G. H. Dieke, *Spectra and Energy Levels of Rare Earth Ions in Crystals* (Interscience, New York, 1968).
[29] J. R. Wietfeldt, D. S. Moore, B. M. Tissue, and J. C. Wright, Phys. Rev. B **33**, 5788 (1986).
[30] B. G. Wybourne, *Spectroscopic Properties of Rare Earths* (Interscience, New York, 1965).
[31] D. S. Moore and J. C. Wright, J. Chem. Phys. **74**, 1626 (1981).
[32] T. Holstein, S. K. Lyo, and R. Orbach, in *Laser Spectroscopy of Solids*, edited by W. M. Yen and P. M. Selzer (Springer-Verlag, Berlin, 1981).